NJC

Accepted Manuscript

This is an *Accepted Manuscript*, which has been through the Royal Society of Chemistry peer review process and has been accepted for publication.

Accepted Manuscripts are published online shortly after acceptance, before technical editing, formatting and proof reading. Using this free service, authors can make their results available to the community, in citable form, before we publish the edited article. We will replace this *Accepted Manuscript* with the edited and formatted *Advance Article* as soon as it is available.

You can find more information about *Accepted Manuscripts* in the Information for Authors.

Please note that technical editing may introduce minor changes to the text and/or graphics, which may alter content. The journal's standard Terms & Conditions and the Ethical guidelines still apply. In no event shall the Royal Society of Chemistry be held responsible for any errors or omissions in this *Accepted Manuscript* or any consequences arising from the use of any information it contains.

ROYAL SOCIETY OF CHEMISTRY

www.rsc.org/njc

Self-regenerative and Self-enhanced Smart Graphene/Ag_3PO_4 Hydrogel Adsorbent under Visible Light

Jie Ma[1,2], Chunyang Chen[1], Fei Yu[1,2,3]**

1 State Key Laboratory of Pollution Control and Resource Reuse, School of Environmental Science and Engineering, Tongji University, 1239 Siping Road, Shanghai 200092, P. R. China. Tel: 86-21-6598 1831; E-mail: jma@tongji.edu.cn

2 Tianjin Key Laboratory of Aquatic Science and Technology, Tianjin Chengjian University, 26 Jinjing Road, Tianjin 300384, China

3 College of Chemistry and Environmental Engineering, Shanghai Institute of Technology, Shanghai 2001418, China; E-mail: fyu@vip.163.com

Abstract

A new self-regenerative and self-enhanced smart adsorbent is synthesized by hybridizing the photocatalyst Ag_3PO_4 nanospheres into the 3D graphene oxide (GO) hydrogel, and then used to absorb and mineralize the artificially synthesized dyes methylene blue (MB) and methyl orange (MO). The results indicate that Ag_3PO_4 particles anchored on the GO sheets densely and firmly with the average diameter of ~20 nm. The large specific surface area (SSA) (~100.29 m^2/g) of the samples could provide many adsorption sites for organic dyes to get good removal effectiveness. The results showed that the 3D graphene/Ag_3PO_4 composites exhibit excellent removal effectiveness of MB and MO as well as reusability. Especially, the adsorption ability of the adsorbent increased greatly after one-time recycling. The negatively charged functional groups of rGO sheets can attract the silver ions (Ag+), which can help the Ag_3PO_4 particles anchored on the rGO sheets. Besides, the rGO hydrogel has adsorption ability toward dyes, which can help increase the contact chance between dyes and nanoparticles Ag_3PO_4. The positive effects between Ag_3PO_4 and GO could be contributed to adsorption activity and photocatalytic properties. This study provides a green way to fabricate self-regenerative and self-enhanced smart hydrogel

adsorbents under visible light.

Keywords: Graphene; Ag_3PO_4; Hydrogel; photocatalysis;

1. Introduction

Many thousands of artificially synthesized dyes are widely used in many industries, such as leather and printing factory, ever since the technique was invented and developed. As a result, much dye wastewater have been discharged[1-3]. At present, removal methods of dye wastewater are mainly divided into chemical, physical, and biological treatment methods[4, 5]. Adsorption method is low cost, simplicity, high efficiency and insensitivity to toxic organic compounds[6-9]. For the reason given above, adsorption is considered to be one of the most effective methods used in wastewater treatment. During the process of adsorption, pollutants continuously accumulate on the adsorbents surface[10]. After saturation, adsorbents turn out to be a hazardous and harmful waste. Thus, it is necessary to dispose of or regenerate them suitably. Disposal of adsorbents as waste is unfriendly to the environment and is uneconomic Because disposable saturation adsorbents are considered to be a waste of resources as well as lead to a significant danger to the environment[11]. Compared to disposition as waste, it is much better to regenerate adsorbents efficiently. Recycling adsorbents would reduce the cost of production as well as emission of waste residue to protect the environment. An excellent regeneration process also requires decomposition of toxic pollutants on the surface of adsorbents and regain the adsorbents' adsorption capacity thus avoiding the secondary pollution.

Regeneration methods can be divided into four major groups: thermal regeneration, chemical regeneration, microbiological regeneration, and vacuum regeneration[12]. Thermal regeneration is the most popularly and widely used method in the industry[13], which heats the saturated adsorbents and provides enough energy necessary to discompose the residual pollutants. The thermal method could utilize hot inert gases and steam to make the adsorbents recover the adsorption ability, such as microwave regeneration, and ultrasound regeneration, etc.[10, 14]. However, there exist some problems such as rigorous energetic requirements and low regeneration efficiency.

Therefore, as alternatives to traditional thermal regeneration, chemical regeneration is developed. Moreover, solvent, wet air, electrochemical, supercritical and thermal oxidative regeneration are considered to be chemical regeneration. Solvent regeneration is easy to implement in practical production process[15], but it cannot completely recover adsorbent's absorbability. Wet air regeneration can achieve good results but needs rigorous requirements for the equipment. Previous reports showed that supercritical regeneration is one of the most efficient methods among all studied[16, 17]. However, its high critical constants (high temperature and high pressure) limit the in-depth investigation and application of this method until now.

For the microbiological regeneration, microbes such as bacteria and yeast are used to degrade the adsorbed organic pollutants, and then the exhausted adsorbents can be regenerated[18]. However, being susceptible to external factors such as temperature and long-lasting times required make the method unfeasible; Vacuum regeneration changes adsorption equilibrium towards desorption by reducing the conditioned pressure. In fact, because this method is only applied to separate and purify gaseous streams, not to regenerate adsorbents [10], and then vacuum regeneration has not yet been employed to develop a true regeneration method. Some reports have been studied to removing CO_2 from the air and air simulating streams by vacuum swing adsorption[19-21].

Given that adsorbents play a core role in the removal of pollutants from wastewater, further investigation of the new-typed and high efficient regeneration method is still necessary. Our group combines chitosan (CS) and the photocatalyst TiO_2 to prepare cross-linking self-regenerative chitosan (SRCS) [12]. The results show that novel SRCS composites possessed high adsorption capacity (~799.2 mg/g) for methyl orange (MO) and excellent self-regenerative advantages. However, as we all known that CS is an organic material, which could be oxidized during the process of photocatalytic self-regeneration. Some reports have reported that graphene oxide(GO) sheets could adsorb organic dyes, such as methylene blue (MB), rhodamine B and acid orange[22] with a relatively high adsorption ability. Ag_3PO_4 photocatalyst has the

excellent photocatalytic ability under visible light irradiation, which could decompose pollutant. Cui et al.[23] showed that graphene oxide (GO)-enwrapped Ag_3PO_4 composites had highly efficient photocatalytic degradation of RhB. Chen Guodong et al.[24] showed that the removal rate of MO is about 86.7% after 50min and RhB solution could be completely degraded within 30 min by Ag_3PO_4/graphene-oxide (Ag_3PO_4/GO) composite. Other reports[25-28] also indicated the GO–Ag_3PO_4 composite had highly efficient and stable visible-light-induced photocatalysts for the removal of organic pollutants Hence, in this paper, we combined the visible-light-driven Ag_3PO_4 photocatalyst and graphene oxide inorganic hydrogel. GO could enhance the contact opportunity of pollutants and Ag_3PO_4. More importantly, GO has excellent electrical performance, which could promote electron transfer and inhibit the recombination of holes (h^+) and electrons (e^-) pairs in the photocatalysts[26], thus improving photocatalytic activity of Ag_3PO_4.

In this paper, we synthesized self-regenerative and self-enhanced smart hydrogel adsorbents(rGO/Ag_3PO_4) by hybridizing the photocatalyst Ag_3PO_4 nanospheres into reduced graphene oxide hydrogel. Then the adsorption activity and photocatalytic properties of the composites were investigated Methylene blue (MB) and methyl orange (MO) were selected as representative target pollutants. Firstly, MB and MO have been adsorbed in the rGO/Ag_3PO4 composites, and then photo-degraded under visible light. More importantly, the new rGO/Ag_3PO4 adsorbent could be recycled easily by filtration and regenerated under visible light, and the adsorption activity could be improved greatly after regeneration. In a word, this study also provides a green way to fabricate self-regenerative and self-enhanced smart hydrogel adsorbents under visible light.

2. Experimental

2.1 Materials

All reagents, such as $AgNO_3$ and KH_2PO_4 were of analytical purity and purchased from Sinopharm Chemical Reagent Co, Ltd. and used in the experiments

directly without any further purification. Deionized water was used in all process of experiments and preparation of the solution.

2.2 Preparation of rGO/Ag_3PO_4 adsorbent

Graphite oxide was dissolved in deionized water to prepare graphite oxide aqueous suspension (2 mg/ml). After ultrasonic exfoliation for 6 h, reduced glutathione (L-GSH) was added to the graphene aqueous suspension, then keeping ultrasonic for 0.5 h to make L-GSH mixed uniformly with graphene. The mixed solution (5 ml) was added into a beaker(10ml), and then heated in water bath at 95℃ for 15 h to prepare graphene oxide hydrogel. The hydrogel was added into $AgNO_3$ aqueous solution (3 ml, 0.1 M) to shake 12 h in the dark to make sure that positively charged Ag^+ can assemble on the surface of negatively charged rGO sheets by electrostatic interaction[29]. Subsequently, the hydrogel adsorbed Ag^+ was added into KH_2PO_4 aqueous solution (3 ml, 0.1 M) to shake for 12 h in the dark, to form nanoparticles Ag_3PO_4 in the inner of the rGO hydrogel, which is named rGO/Ag_3PO_4 adsorbent.

2.3 Batch adsorption experiments

The adsorption of MO or MB could reach equilibrium after the contact time of 3 days in preliminary experiments. Therefore, 3 days were selected as adsorption time. The two parallel adsorption experiments were carried out by putting rGO/Ag_3PO_4 adsorbents (10 mg GO in the rGO/Ag_3PO_4 adsorbents) and 40 ml dye solution of 50mg/L of MO and MB, respectively in 50 ml glass bottles, in the dark for 3 days.At the same time, the blank experiments without the addition of rGO/Ag_3PO_4 adsorbents were conducted to confirm that the decrease in the concentration was mainly contributed to rGO/Ag_3PO_4 adsorbents，instead of other materials such as glass bottles wall.Then the concentration of dye in the aqueous solution got by UV spectrophotometer according to the maximum absorbance peaks of dyes (λ_{max}=465 nm for MO and λ_{max}=665 nm for MB) The average values were analyzed. A calibration curve was carried out to describe the relation between absorbance and

concentration of the dye in terms of Beer-Lambert's law. For high concentration, the dye solutions were diluted with deionized water.

The adsorption capacity dye on adsorbents (q_t mg/g) was defined as follows:

$$q_t = (C_0 - C_t) \times \frac{V}{m} \qquad (1)$$

where c_0 and c_t are the initial dye concentrations and equilibrium concentrations (mg/L), V is the solution volume (L); and m is a adsorbent weight (g)[30].

2.4 Regeneration process

After absorbing the organic dyes (MB and MO, 50 mg/L) for 3 days, adsorbents turned to be saturated. The saturated adsorbents were put in deionized water (40 mL), then irradiated under visible-light illumination (1000 W Xenon Lamp, Shanghai) at ambient temperature for 1 h, finally put in an aqueous solution of organic dyes (MB and MO, 50 mg/L) for a new adsorption as a self-regenerative adsorbent.

2.5 Characterization methods

The morphology characteristics and feature of the rGO/Ag_3PO_4 adsorbents were investigated by transmission electron microscopy (TEM, JEOL Japan) with EDX analysis. X-Ray diffraction (XRD) experiments were conducted by using a X-ray diffractometer (Bruker D8 Advance, Bruker AXS, Germany)With Nickel-filtered Cu $_{Ka}$ radiation The specific surface area (SSA) and pore structure of samples were analyzed from the adsorption/desorption isotherms of N_2 at 77K by multi-point BET and Barrett-Joyner-Halenda (BJH) method. The information of phase and crystallinity can get from X-Ray photoelectron spectroscopy (XPS) by a Kratos Axis Ultra DLD spectrometer, using monochromated Al Ka X-rays. The weight of Ag_3PO_4 anchored on rGO are estimated by thermogravimetric (TG) and Differential Scanning Calorimetry (DSC) analysis by TA Instruments® Q600 SDT thermal analyzer TG and DSC curves were obtained by heating approximately 10 mg of finely samples from 50 to 1000 °C at a heating rate of 10 °C/min in air.

3 Results and discussion

As shown in Fig. 1, reduced graphene oxide（rGO）hydrogel was fabricated by putting the prepared GO solution in a water bath at 95℃ for 15 h. The hydrogel was added into $AgNO_3$ aqueous solution and KH_2PO_4 aqueous solution, successively, finally getting the smart rGO/Ag_3PO_4 adsorbent. Then the novel adsorbents were put in organic dyes solution. After absorbing dyes for 3 days, adsorbents turned to be saturated. The saturated adsorbent was irradiated under visible-light illumination for 1h to regenerate the adsorbents. The process of adsorption and regeneration can be recycled in the same way given above.

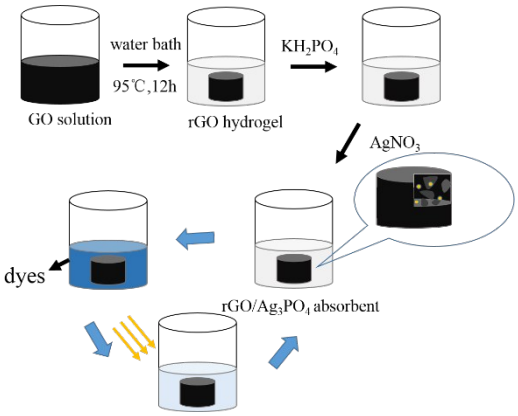

Fig. 1. Schematic diagram of adsorption and photocatalytic regeneration of rGO/Ag_3PO_4 composites

3.1 Characterization of graphene/Ag_3PO_4 composites

Firstly, the morphology and structure of the samples were investigated by TEM and SEM images, as shown in Fig. 2. It can be clearly seen that the light-gray films are the reduced graphene oxide sheets, and the black spots with the average diameter of 20 nm are considered as Ag_3PO_4 nanoparticles. Apparently, Ag_3PO_4 particles anchored on the rGO sheets densely and firmly even after extensive sonication by ultrasound to disperse before TEM characterization[31]. During the synthesis of rGO/Ag_3PO_4 composites, the negatively charged functional groups of rGO sheets can attract the silver ions (Ag^+), and then forming particles when eventually KH_2PO_4 adding into the solution[26], which is in good accord with the reports that rGO sheets could act as a support [32, 33]. Besides, Ag_3PO_4 located on rGO hydrogel could be further verified by

EDS analysis in Fig. 2d, which shows the coexistence of C, O, P and Ag in the reduced graphene oxide hydrogel. The element C originates from GO. The atomic ratio of P and Ag is 0.9: 3.47, which is close to the chemical composition of Ag_3PO_4. The content of the rGO/Ag_3PO_4 composites was calculated to be around 30 wt % in terms of EDS analysis. The selected-area electron diffraction(SAED) pattern of Ag_3PO_4 was added, as shown in the Fig 2c. The diffuse rings of SAED pattern indicate the polycrystalline structure of Ag_3PO_4 nanoparticles, which could be indexed to the (220), (421), (422) of cubic Ag_3PO_4 phase[34]. Besides, from the SEM(Fig. 2e, f), we could easily observe the porous structure of rGO/Ag_3PO_4 composites. The excellent feature could promote the adsorption of dyes.

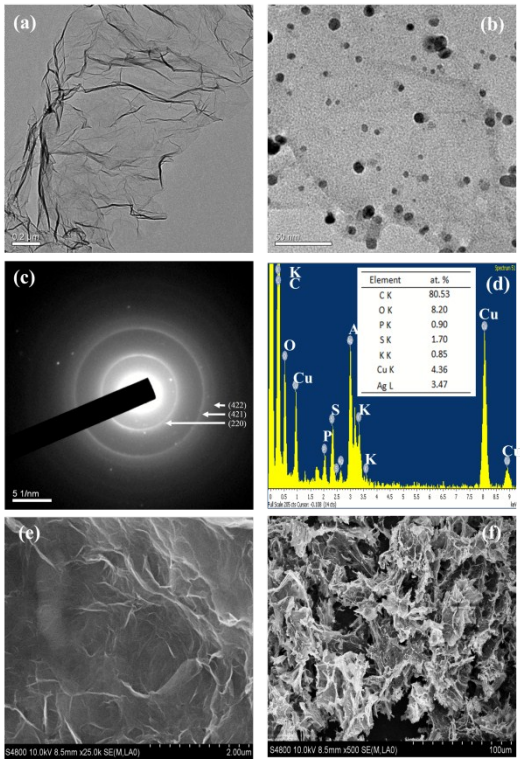

Fig. 2 TEM images of graphene (a) and rGO/Ag_3PO_4 composites (b), SAED images (c), the EDS pattern (d) of Ag_3PO_4 and SEM images (e, f) of rGO/Ag_3PO_4 composites

Fig. 3a displays the TG and DSC curves, indicating that the amount of Ag_3PO_4 in the samples can be estimated at around 30 wt% in accordance with EDS analysis of TEM. The weight loss below 110℃ on the samples was regarded as the desorption of surface water[35]. A rapid weight loss from 180 ℃ and 200 ℃ on the samples could

be due to combustion of GSH. The weight loss before 600 ℃ was attributed to decomposition and combustion of oxygen-containing groups[36], for different oxygen-containing groups have different temperatures of decomposion[37]. The clear step of mass loss at 638.2 ℃ is owing to complete oxidization of the carbon framework[36]. After 650 ℃, the samples weight stabilized around 30 wt%, which could be the amount of Ag_3PO_4. The TG curve (a) of graphite oxide was also analyzed in the Fig. S1 (EIS). The graphite oxide turns into graphene oxide after ultrasonic exfoliation for 6h. Therefore, the TG of graphite oxide could represent the TG of graphene oxide to some extent. The XRD analysis was carried out to confirm the Ag_3PO_4 nanoparticles anchored on the rGO hydrogel. The XRD patterns of GO, rGO hydrogel, as-prepared bare Ag3PO4, rGO/Ag_3PO_4 composites are shown in Fig. 3b. From the pattern of GO and rGO hydrogel, the obvious peaks at around 2θ=10.92° and 2θ=23.8 ° can be found, respectively, showing that the GO was reduced by L-GSH into rGO[38]. Then the XRD pattern of bare Ag_3PO_4 could be well-judged to the body-centered cubic structure (JCPDS card No.06-0505). Compared with the XRD pattern of bare Ag_3PO_4, some similar peaks of bare Ag_3PO_4 can be found in the XRD pattern of rGO/Ag_3PO_4 composites, confirming that the Ag_3PO_4 nanoparticles anchored on the rGO hydrogel.

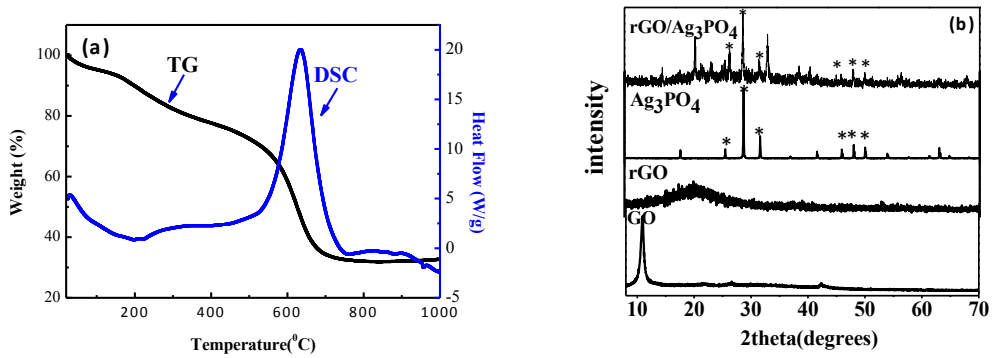

Fig. 3. TG and DSC curve (a) and XRD pattern (b) of the rGO/Ag_3PO_4 composite

The specific surface area (SSA) of the samples might play an important role in the process of reaction[39]. A large SSA could provide more adsorption sites for organic dyes, increasing the contact opportunities between organic dyes and photocatalyst

Ag_3PO_4 in the composites, finally achieving excellent removal of MB and MO. Therefore, the SSA and the corresponding pore size characterization of samples were performed by nitrogen (77.4K) adsorption/desorption experiments samples, as shown in Fig. 4. The SSA of the samples in this work is 100.29 m^2/g, much more than the nanosized particles-graphene composite (18.7 m^2/g) prepared by Xiang et al.[25], which could facilitate the high adsorption ability towards organic dyes and high removal of dyes. Besides, the detailed information about the pore-distribution analysis is presented in Table 1

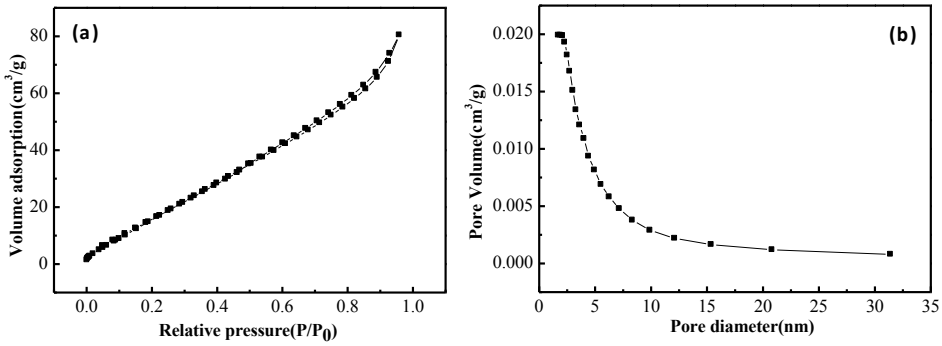

Fig. 4. N_2 adsorption/desorption isotherms (a) and pore size distribution (b) of rGO/Ag_3PO_4 composite

Table 1 Physical properties of rGO/Ag_3PO_4 adsorbentss

Surface area(m^2/g)	Average pore size(nm)	Pore volume(cm^3/g)
100.29	4.95	0.119

The XPS analysis was also carried out to ascertain further the chemical status of the composition, and then to validate Ag_3PO_4 bound to the graphene oxide hydrogel. As shown in Fig. 5b. The peaks at 374.63 and 368.58 eV are due to the binding energies of the Ag3d5/2 and Ag3d3/2 of Ag^+, respectively, which confirmed the existence of Ag^+ in Ag_3PO_4[40]. The binding energies of the peak at 133.73 eV is corresponding to P^{5+} of PO_4^{3-} in Fig. 5c. From the Fig. 5d, the peak C1s at 284.83eV of the simple is due to functional groups in GO[29], which can be attributed to four functional groups as follows: C-C (284.7eV), C-O (285.6eV), C=O (286.5eV),

O-C=O(288.2eV), respectively. As shown in Fig. 5d, four characteristic peaks of C-C, C-O, C=O, O-C=O can be obviously seen in the XPS e spectrum of C1s for the samples [29]. The appearance of Ag3d peaks and P^{5+} peak also indicates that the Ag_3PO_4 nanoparticles were located in rGO hydrogel during the synthesis process of samples.

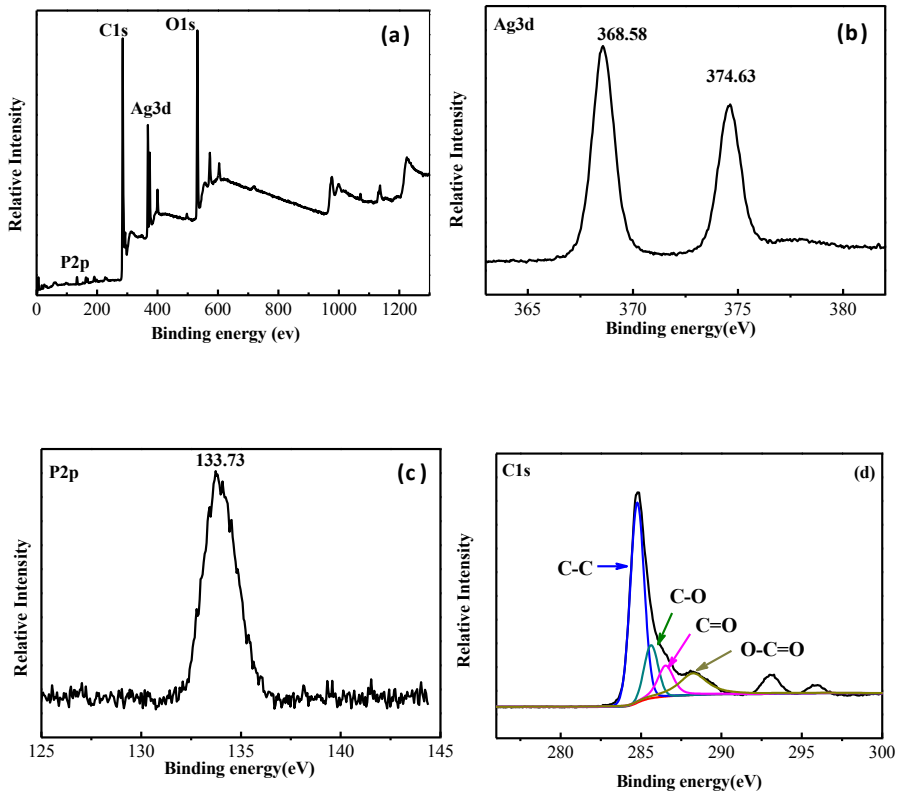

Fig. 5 XPS survey spectra (a), the Ag_{3d} region (b), P_{2p} region (c), and C_{1s} region of the rGO/Ag_3PO_4 composite.

3.2 Renegeration performance under visible light

As mentioned above, it is reasonably expected that the prepared samples may have excellent adsorptive and degradation performance of organic dyes and self-regenerative ability because graphene oxide(GO) sheets could adsorb organic dyes with a relatively high adsorption ability. Moreover, the photocatalyst Ag_3PO_4 can decompose the organic compounds such as dyes under the irradiation of visible light. To study the adsorption mechanism, the adsorption isotherm and adsorption kinetics

toward MB have been added in the paper. Adsorption isotherm and parameters as shown in Fig. S2 and Table S1(ESI) describes the interaction between solution and adsorbent[41]. As shown in Fig. S2 (ESI), the result was analyzed by Langmuir and Freundlich isotherm models, respectively. We could find that the process of adsorption obeys well the Langmuir isotherm that could be regarded as chemical adsorption. The experimental results at various times were fitted by pseudo-first order model and pseudo-second order model, in Fig. S3 (b,c). The kinetic parameters of pseudo first- and second-order adsorption kinetic models for MB on rGO/Ag3PO4 composite could be found in Table S2 (ESI). The fact the correlation coefficient (R^2=0.9494) of pseudo-first order kinetic model (R^2=0.7084) is greater than the pseudo-second order suggests the process of adsorption follow the pseudo-first-order model.

To investigate the practical application of the as-obtained new adsorbent, blank test and cycling degradation experiments were conducted to investigate further the recyclability, as shown in Fig. 6.

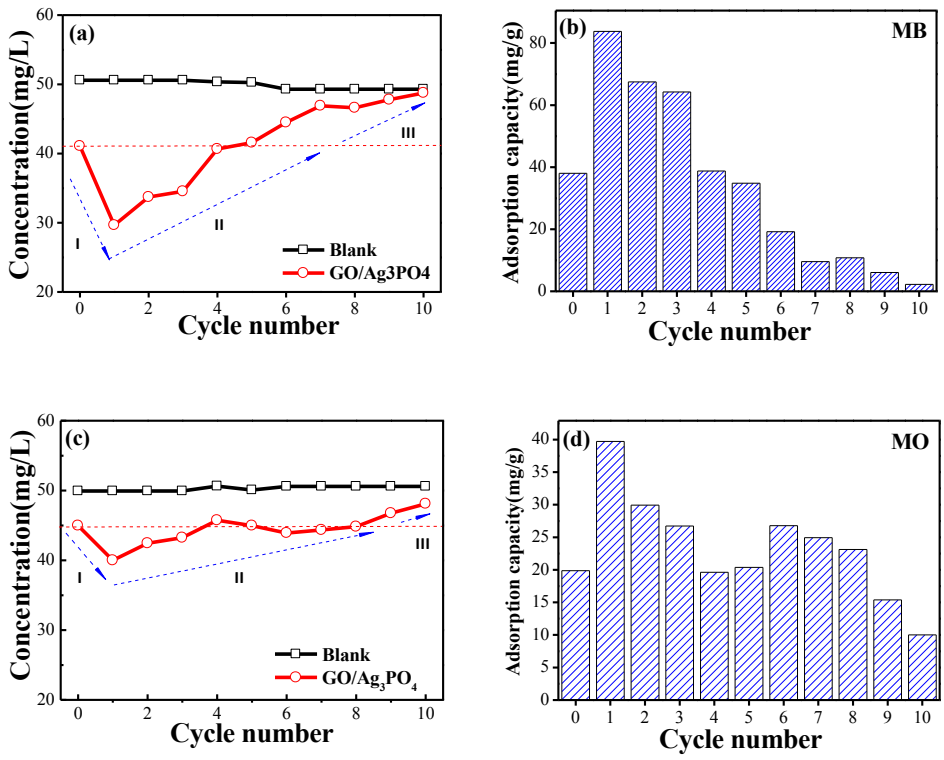

Fig. 6. The removal ability and adsorption reusability of MB (a, b) and MO (c, d) on the rGO/Ag_3PO_4 composite

We could also find that the prepared samples exhibit relatively high affinity for cationic dyes MB, but low adsorption for anionic dyes MO, which can be contributed to the large negative charge density of GO with various oxygen-containing groups[42]. More interesting, it was observed that the adsorption ability of the new adsorbent recycled once increased greatly (adsorption capacity of MB from 38.04 mg/g to 83.75 mg/g, the adsorption capacity of MO from 19.87 mg/g to 39.72 mg/g), as shown in stageI in Fig. 6. The enhanced adsorption ability of the new adsorbent after once recycling,such as the removal rate of MB and MO after once recycle improve 23% and 10%, in the initial concentration ~50mg/L, respectively. The enhanced performance can be due to the following reasons: Firstly, the structure of 3D rGO hydrogel might be changed by Ag^+ because of its strong oxidability, adding the specific surface area (SSA) of the composite. Second, as shown in Fig. 7a and 7b, nanoparticles Ag_3PO_4 decomposed into smaller nanoparticles Ag during the photocatalysis, lead to an increase of the SSA. Furthermore, the nanoparticles Ag can also transfer the photogenerated electrons, inhibiting the recombination of electron-hole pairs and promoting the photocatalytic ability[40]. However, from the Fig. 7b, we can find the with the further increase of recycle times, the photocatalytic ability decreases, Because the photo corrosion of Ag_3PO_4 lead to more nanoparticles Ag on the surface of the Ag_3PO_4 when cycling the rGO/ Ag_3PO_4 adsorbent again and again, so that hindering the contact between Ag_3PO_4 and dyes and reducing the amount of photocatalyst, thus reducing the photocatalytic ability, as shown in Fig. 7c. Nevertheless, after 10 runs the new adsorbent still had photocatalytic activity, indicating the composite material has good photocatalytic degradation efficiency of MB and MO. The synergistic effects[26] between adsorption ability of rGO hydrogel and photocatalytic activity of Ag_3PO_4 facilitate the photodegradation of the organic dyes MB and MO. Meanwhile, the rGO hydrogel can also accept photoexcited electrons and inhibit the recombination of electron-hole pairs[33, 43-46] during the process

of photodegradation due to the anti-bonding π* orbital of rGO (-0.75eV) lower than that of hydrogen (-0.046eV). As well known, previous investigations and reports[29, 31] give the mechanism of photodegradation: As shown in Fig. 8a, when the rGO/Ag_3PO_4 composite was irradiated with visible light, the valence band (VB) electrons (e^-) of photocatalysis could be motivated to the conduction band (CB), then transferring to the rGO sheets of the composite, leaving the holes (h^+) in VB. The photogenerated electron can react with surface O_2 to produce reactive oxygen species(O_2^-). The holes (h^+) and O_2^- have strong oxidability, which can react with H_2O to form active radical species ·OH. Then ·OH can decompose MB and MO into CO_2, H_2O, and other mineralization product[47]. Meanwhile, even if the GO sheets can transfer the photogenerated electrons and suppress the recombination of electrons and holes, it still is inevitable for Ag_3PO_4 to decompose into metallic Ag[31], thus, reducing the photocatalytic ability. As shown in Fig. 8b, which is corresponding to the regeneration process stage II， the photogenerated electrons transfer to the rGO sheets and Ag nanoparticles, and then the electrons on the Ag nanoparticles can also transfer quickly to the rGO sheets, thus suppressing the recombination of electrons and holes.

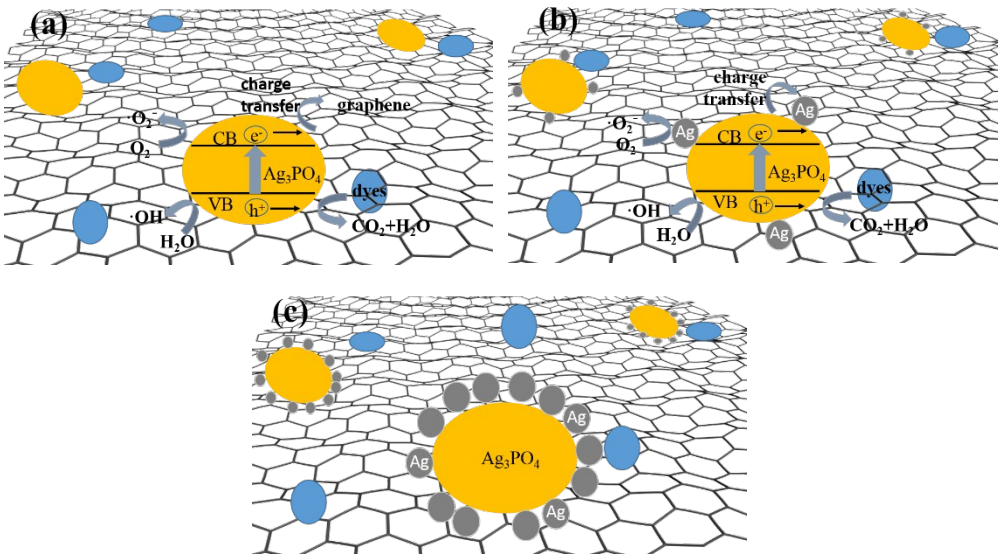

Fig. 7 Ag_3PO_4 photocatalysis regeneration process: stage I (a), stage II (b), and stage III (c)

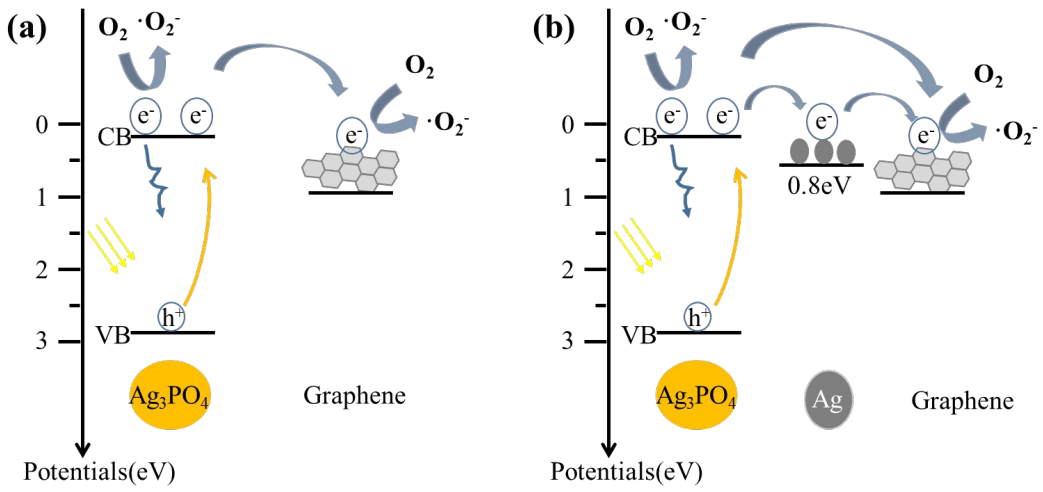

Fig. 8 The energy band diagram corresponding to regeneration process stage I (a), and stage II (b)

4. Conclusion

In this work, we prepared a new adsorbent by introduced photocatalyst Ag_3PO_4 into 3D reduced graphene oxide hydrogel, which makes it easy to be removed by filtration and be recycled by visible light. The resulting 3D reduced graphene oxide/Ag_3PO_4 composite adsorbents exhibit excellent removal effectiveness of methylene blue (MB) and methyl orange (MO). As well as reusability, especially for one-time recycling under visible light. The present prepared adsorbents could not be reused many times with poor recycling ability. Therefore, the design of stabilized rGO-based hydrogel composites is still a challenge in the future. Hence, the current research work provides a green way to fabricate self-regenerative and self-enhanced smart hydrogel adsorbents under visible light.

Acknowledgment

This research was supported by the National Natural Science Foundation of China (No. 21577099, 51408362), the Research Fund of Tianjin Key Laboratory of Aquatic Science and Technology (No. TJKLAST-ZD-2014-07), State Key Laboratory of Pollution Control and Resource Reuse Foundation (No. PCRRF14021), and the Fundamental Research Funds for the Central Universities.

Reference

1. H. El Boujaady, A. El Rhilassi, M. Bennani-Ziatni, R. El Hamri, A. Taitai and J. L. Lacout, *Desalination*, 2011, **275**, 10-16.
2. J. Ma, F. Yu, L. Zhou, L. Jin, M. Yang, J. Luan, Y. Tang, H. Fan, Z. Yuan and J. Chen, *ACS applied materials & interfaces*, 2012, **4**, 5749-5760.
3. F. Yu, J. Chen, L. Chen, J. Huai, W. Gong, Z. Yuan, J. Wang and J. Ma, *Journal of colloid and interface science*, 2012, **378**, 175-183.
4. Y. M. Slokar and A. M. Le Marechal, *Dyes and Pigments*, 1998, **37**, 335-356.
5. O. J. Hao, H. Kim and P. C. Chiang, *Critical Reviews in Environmental Science and Technology*, 2000, **30**, 449-505.
6. V. K. Gupta and I. Ali, *Environmental Science & Technology*, 2008, **42**, 766-770.
7. V. K. Gupta, B. Gupta, A. Rastogi, S. Agarwal and A. Nayak, *Journal of Hazardous Materials*, 2011, **186**, 891-901.
8. V. K. Gupta, A. Mittal, V. Gajbe and J. Mittal, *Journal of Colloid and Interface Science*, 2008, **319**, 30-39.
9. V. K. Gupta, A. Mittal, A. Malviya and J. Mittal, *Journal of Colloid and Interface Science*, 2009, **335**, 24-33.
10. F. Salvador, N. Martin-Sanchez, R. Sanchez-Hernandez, M. J. Sanchez-Montero and C. Izquierdo, *Microporous and Mesoporous Materials*, 2015, **202**, 277-296.
11. F. Yu, L. Chen, J. Ma, Y. R. Sun, Q. Li, C. L. Li, M. X. Yang and J. H. Chen, *Rsc Advances*, 2014, **4**, 5518-5523.
12. F. Yu, L. Chen, J. Ma, Y. Sun, Q. Li, C. Li, M. Yang and J. Chen, *Rsc Advances*, 2014, **4**, 5518-5523.
13. S. W. Nahm, W. G. Shim, Y. K. Park and S. C. Kim, *Chemical Engineering Journal*, 2012, **210**, 500-509.
14. F. Salvador, N. Martin-Sanchez, R. Sanchez-Hernandez, M. J. Sanchez-Montero and C. Izquierdo, *Microporous and Mesoporous Materials*, 2015, **202**, 259-276.
15. D. S. Guo, Q. T. Shi, B. B. He and X. Y. Yuan, *Journal of Hazardous Materials*, 2011, **186**, 1788-1793.
16. M. J. Sanchez-Montero, F. Salvador-Palacios, A. Salvador-Palacios and M. J. Martin-Rodriguez, in *Advanced Materials Forum Iii, Pts 1 and 2*, ed. P. M. Vilarinho, 2006, vol. 514-516, pp. 1742-1747.
17. F. Salvador, N. Martin-Sanchez, M. J. Sanchez-Montero, J. Montero and C. Izquierdo, *Journal of Supercritical Fluids*, 2013, **74**, 1-7.
18. R. L. Zhu, J. X. Zhu, F. Ge and P. Yuan, *Journal of Environmental Management*, 2009, **90**, 3212-3216.
19. R. Thiruvenkatachari, S. Su, X. X. Yu and J. S. Bae, *International Journal of Greenhouse Gas Control*, 2013, **13**, 191-200.
20. M. G. Plaza, S. Garcia, F. Rubiera, J. J. Pis and C. Pevida, *Chemical Engineering Journal*, 2010, **163**, 41-47.
21. E. Kikkinides, R. Yang and S. Cho, *Industrial & Engineering Chemistry Research*, 1993, **32**, 2714-2720.

22. Z. G. Xiong, L. L. Zhang, J. Z. Ma and X. S. Zhao, *Chemical Communications*, 2010, **46**, 6099-6101.
23. H. Cui, X. Yang, Q. Gao, H. Liu, Y. Li, H. Tang, R. Zhang, J. Qin and X. Yan, *Materials Letters*, 2013, **93**, 28-31.
24. G. Chen, M. Sun, Q. Wei, Y. Zhang, B. Zhu and B. Du, *Journal of Hazardous Materials*, 2013, **244**, 86-93.
25. Q. Xiang, D. Lang, T. Shen and F. Liu, *Applied Catalysis B-Environmental*, 2015, **162**, 196-203.
26. L. Liu, J. C. Liu and D. D. Sun, *Catalysis Science & Technology*, 2012, **2**, 2525-2532.
27. X. Yang, J. Qin, Y. Jiang, R. Li, Y. Li and H. Tang, *Rsc Advances*, 2014, **4**, 18627-18636.
28. X. Yang, J. Qin, Y. Jiang, K. Chen, X. Yan, D. Zhang, R. Li and H. Tang, *Applied Catalysis B-Environmental*, 2015, **166**, 231-240.
29. X. F. Yang, H. Y. Cui, Y. Li, J. L. Qin, R. X. Zhang and H. Tang, *Acs Catalysis*, 2013, **3**, 363-369.
30. F. Yu, Y. Q. Wu and J. Ma, *Journal of Hazardous Materials*, 2012, **237**, 102-109.
31. Q. H. Liang, Y. Shi, W. J. Ma, Z. Li and X. M. Yang, *Physical Chemistry Chemical Physics*, 2012, **14**, 15657-15665.
32. R. Pasricha, S. Gupta and A. K. Srivastava, *Small*, 2009, **5**, 2253-2259.
33. M. Zhu, P. Chen and M. Liu, *Acs Nano*, 2011, **5**, 4529-4536.
34. Q. Liang, W. Ma, Y. Shi, Z. Li and X. Yang, *Crystengcomm*, 2012, **14**, 2966-2973.
35. S. Z. Liu, H. Q. Sun, S. M. Liu and S. B. Wang, *Chemical Engineering Journal*, 2013, **214**, 298-303.
36. H. Q. Sun, S. Z. Liu, S. M. Liu and S. B. Wang, *Applied Catalysis B-Environmental*, 2014, **146**, 162-168.
37. J. L. Figueiredo, M. F. R. Pereira, M. M. A. Freitas and J. J. M. Orfao, *Carbon*, 1999, **37**, 1379-1389.
38. P. Tuan Anh, J. S. Kim, J. S. Kim and Y. T. Jeong, *Colloids and Surfaces a-Physicochemical and Engineering Aspects*, 2011, **384**, 543-548.
39. M. H. Cao, P. F. Wang, Y. H. Ao, C. Wang, J. Hou and J. Qian, *International Journal of Hydrogen Energy*, 2015, **40**, 1016-1025.
40. W. G. Wang, B. Cheng, J. G. Yu, G. Liu and W. H. Fan, *Chemistry-an Asian Journal*, 2012, **7**, 1902-1908.
41. V. M. Vucurovic, R. N. Razmovski and M. N. Tekic, *Journal of the Taiwan Institute of Chemical Engineers*, 2012, **43**, 108-111.
42. S. Wang, H. Sun, H. M. Ang and M. O. Tade, *Chemical Engineering Journal*, 2013, **226**, 336-347.
43. J. Liu, H. Bai, Y. Wang, Z. Liu, X. Zhang and D. D. Sun, *Advanced Functional Materials*, 2010, **20**, 4175-4181.
44. T. Xu, L. Zhang, H. Cheng and Y. Zhu, *Applied Catalysis B-Environmental*, 2011, **101**, 382-387.
45. M. L. Li, Y. J. Zhang and Q. H. Xu, *Chinese J Inorg Chem*, 2010, **26**, 2033-2040.
46. M. S. Zhu, P. L. Chen and M. H. Liu, *Chinese Science Bulletin*, 2013, **58**, 84-91.
47. M. R. Hoffmann, S. T. Martin, W. Y. Choi and D. W. Bahnemann, *Chemical Reviews*, 1995, **95**, 69-96.

Graphical Abstract

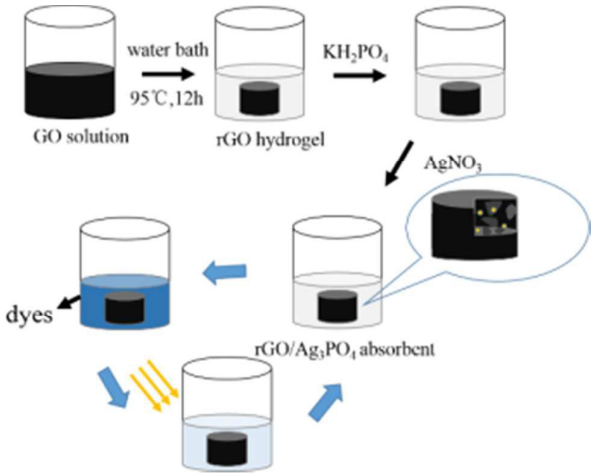

We prepared a new 3D adsorbent which makes it easy to be removed by filtration and be recycled.